

## Two distinct patterns of spring Eurasian snow cover anomaly and their impacts on the East Asian summer monsoon

So-Young Yim,<sup>1,2</sup> Jong-Ghap Jhun,<sup>3</sup> Riyu Lu,<sup>4</sup> and Bin Wang<sup>2</sup>

Received 2 February 2010; revised 5 August 2010; accepted 18 August 2010; published 23 November 2010.

[1] The Eurasian snow cover anomaly in spring has been considered as one of the important factors affecting East Asian summer monsoon (EASM). The spring snow cover data for the period from 1972 to 2004 are used to extract dominant spatial patterns over the Eurasian region and to examine their impacts on the EASM through empirical orthogonal function (EOF) analysis. The first EOF mode is generally characterized by a continent-wide snow cover anomaly over the whole Eurasian region, while the second EOF mode is dominated by an east-west dipole structure over Eurasia. Our study indicates that the variability of dipole pattern snow cover is more closely related to the EASM rainfall than that of continent-wide snow cover. A strong dipole pattern with positive (negative) snow cover anomalies over western Eurasia and negative (positive) snow cover anomalies over eastern Eurasia signifies enhanced (reduced) summer rainfall over East Asia, and the Eurasian wave train pattern is apparent. An important implication of these results is that the spring snow cover anomaly over Eurasia provides a complementary precursor for EASM variability.

**Citation:** Yim, S.-Y., J.-G. Jhun, R. Lu, and B. Wang (2010), Two distinct patterns of spring Eurasian snow cover anomaly and their impacts on the East Asian summer monsoon, *J. Geophys. Res.*, 115, D22113, doi:10.1029/2010JD013996.

### 1. Introduction

[2] The year-to-year variation of the East Asian summer monsoon (EASM) is one of the most challenging and important tasks in climate prediction. The interannual variability of EASM is affected by anomalous states of lower boundary condition such as sea surface temperature (SST), snow cover/snow depth, and soil moisture [Charney and Shukla, 1981]. Among them, the snow cover/snow depth may have an important effect on the interannual variability of the monsoon because of its ability to alter the surface albedo and to regulate the soil moisture [Hahn and Shukla, 1976; Barnett et al., 1989; Yasunari et al., 1991; Sankar-Rao et al., 1996; Kripalani et al., 2003].

[3] Two large areas with snow can be seen over the Tibetan Plateau (TP) and the Eurasian region in winter and spring (Figure 1). For this reason, relationships between the TP snow cover/snow depth and EASM have been studied [Chen and Wu, 2000; Wu and Qian, 2003; Zhang et al., 2004; Zhao et al., 2007]. The linkages between the Eurasian snow cover/snow depth and EASM have been also

studied, but there are relatively fewer observational studies about the influence of Eurasian snow on the EASM compared to the Indian summer monsoon (ISM). In the influence of Eurasian snow on ISM, observational studies showed that there generally exists an inverse relationship between interannual variations of the snow cover/snow depth over Eurasia and the ISM, indicating that excessive (deficient) Eurasian snow cover/snow depth in winter to spring is followed by a weak (strong) ISM rainfall [Hahn and Shukla, 1976; Kripalani et al., 1996; Sankar-Rao et al., 1996; Bamzai and Shukla, 1999]. To confirm the inverse snow-ISM rainfall relationship and to examine the influence of Eurasian snow depth on the Asian summer monsoon circulation, Dash et al. [2006a] conducted sensitivity experiments using spectral general circulation model (GCM) of Indian Institute of Technology, Delhi. They revealed an increase ISM rainfall in response to less snow depth over Eurasia. Other model simulations of the global climate system have also indicated that an inverse relationship exists between the snow on the Eurasian continent and the ISM rainfall [Barnett et al., 1989; Bamzai and Marx, 2000; Dash et al., 2006b].

[4] On the other hand, in the influence of Eurasian snow on the EASM, Yang and Xu [1994] found that the Eurasian winter snow cover is positively correlated with the summer rainfall in northern and southern China, while the snow cover is negatively correlated in central, northeastern, and western China. Liu and Yanai [2002] found that large Eurasian snow cover in spring leads to cooling and a cyclonic circulation anomaly in the lower troposphere over Eurasia, forming a Rossby wave train response and then leading to below-normal EASM rainfall. Kripalani et al.

<sup>1</sup>Research Institute of Basic Sciences, Seoul National University, Seoul, South Korea.

<sup>2</sup>International Pacific Research Center, University of Hawai'i at Manoa, Honolulu, Hawaii.

<sup>3</sup>School of Earth and Environmental Sciences and Research Institute of Oceanography, Seoul National University, Seoul, South Korea.

<sup>4</sup>Institute of Atmospheric Physics, Chinese Academy of Sciences, Beijing, China.

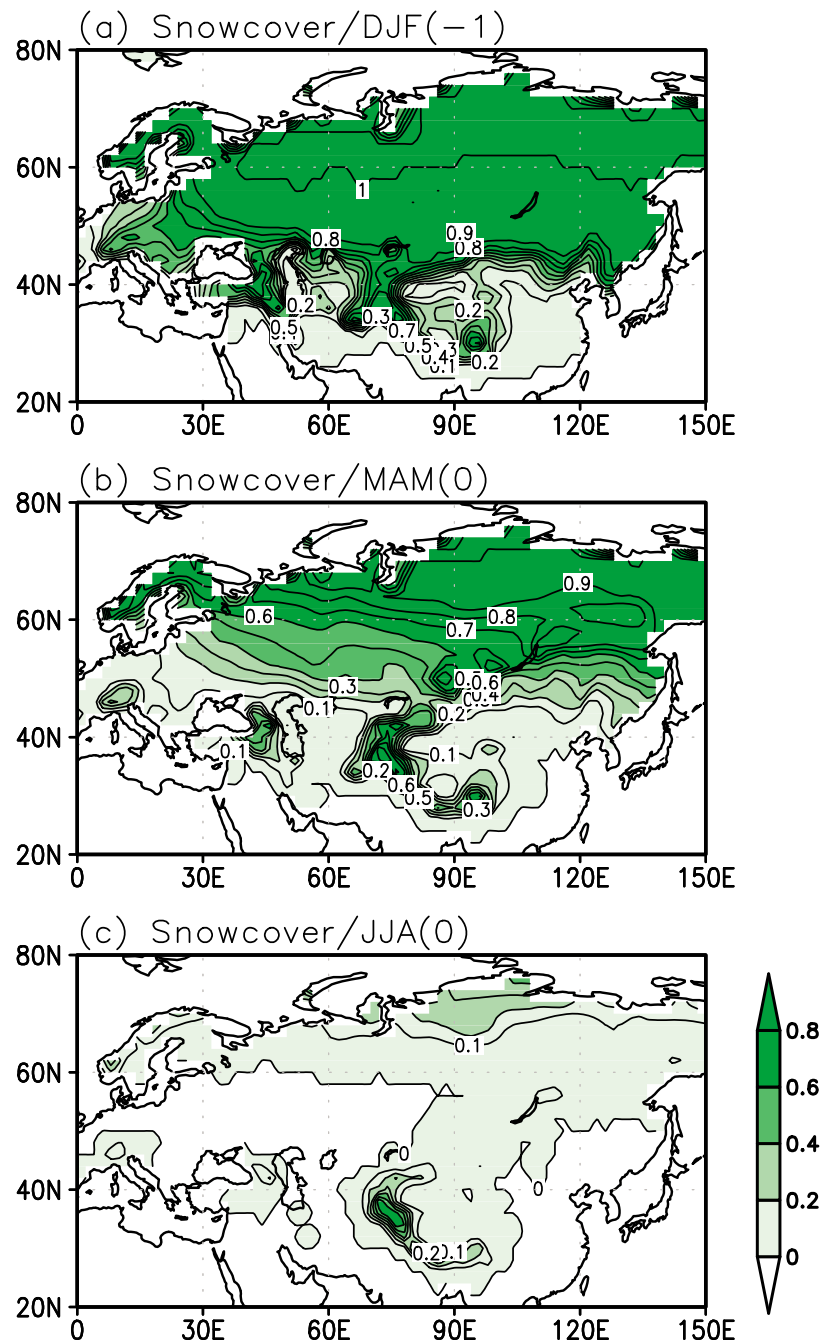


**Figure 1.** Climatological mean fields of the snow cover in (a) winter, (b) spring, and (c) summer. The contour interval is 0.1.

[2002] showed that winter/spring snow depth over western Eurasia is negatively related, whereas the snow depth over eastern Eurasia is positively related with Korean monsoon rainfall. *Wu and Kirtman* [2007] found that spring rainfall variations in southern China are positively correlated with an anomalous spring snow cover in western Siberia, whereas summer rainfalls are weakly correlated with spring Eurasian snow cover. The above studies indicate that anomalous snow variability is seen in the whole Eurasia, the western Eurasia, and the eastern Eurasia. Furthermore, *Dash*

*et al.* [2005] found that snow anomalies are often opposite over the western Eurasia and the eastern Eurasia. Therefore, in our study, we identify dominant patterns of spring snow cover anomaly over Eurasia through empirical orthogonal function (EOF) analysis and examine their impacts on rainfall and circulation fields over East Asia in spring and summer. The data sets used in our study are described in section 2. In section 3, the variability of snow cover is presented. Two dominant modes of spring snow cover over Eurasia and their influences on the EASM are shown in

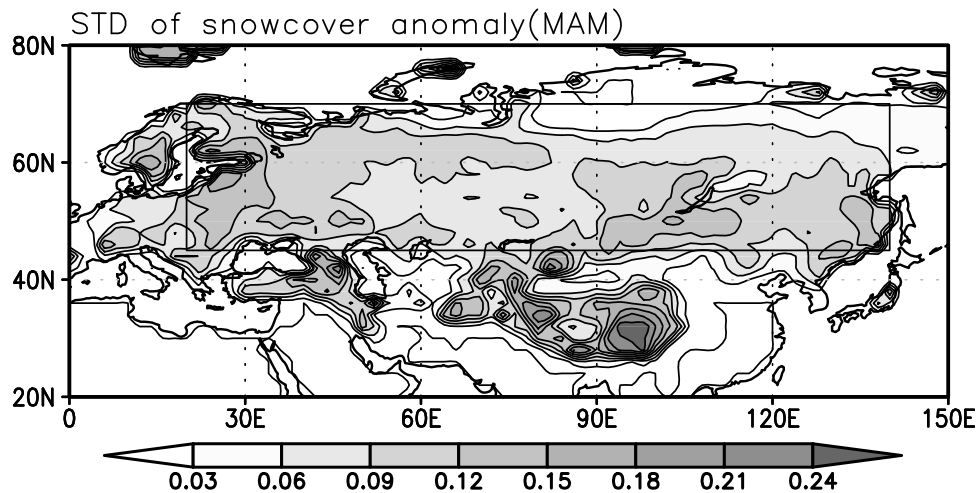


**Figure 2.** The standard deviation (STD) of spring snow cover anomaly. The box indicates the Eurasian region ( $45^{\circ}\text{N}$ – $70^{\circ}\text{N}$ ,  $20^{\circ}\text{E}$ – $140^{\circ}\text{E}$ ) used in our study.

section 4 and section 5, respectively. The summary and discussions are given in section 6.

## 2. Data

[5] The observed data used in this study are obtained from the monthly mean reanalysis data set of the National Centers for Environmental Prediction–National Center for Atmospheric Research (NCEP–NCAR) [Kalnay *et al.*, 1996], global land precipitation (PREC/L) monthly precipitation data of the National Oceanic and Atmospheric Administration (NOAA) [Chen *et al.*, 2002], and the Climate Prediction Center (CPC) Merged Analysis of Precipitation (CMAP) data set [Xie and Arkin, 1997]. The resolution of the NCEP–NCAR reanalysis data is 2.5 degree in latitude and longitude along with 12 pressure levels from 1000 to 100 hPa and the PREC/L precipitation data have spatial resolution of 2.5 by 2.5 degrees for the period from 1972 to 2004.

[6] The snow cover data are derived from NOAA satellites and compiled at the National Environmental Satellite, Data, and Information Service. These data consist of weekly snow cover data, which indicate only the presence or the absence of snow in the Northern Hemisphere. The original  $89 \times 89$  data grid spaced on a polar stereographic projection are converted to a  $180 \times 45$  data grid with a  $2^{\circ} \times 2^{\circ}$  resolution in the Northern Hemisphere from  $20^{\circ}\text{N}$  to  $90^{\circ}\text{N}$ . The interannual variability of snow cover at a point is measured by the interannual variability of the frequency of occurrence of snow at the grid point.

## 3. Variability of Snow Cover

[7] Figure 1 shows the climatology of snow cover in winter, spring, and summer for the period of 1972–2004. There are two main snow cover areas which are located in the TP and Eurasian region. The western part of TP has high snow coverage due to high elevation, but the snow coverage over the eastern part of TP decreases from the previous winter to summer. In the region north of  $45^{\circ}\text{N}$  winter snow covers more than 90% of the total areas. This snow cover shrinks rapidly in spring and exhibits a large meridional

gradient between  $45^{\circ}\text{N}$  and  $70^{\circ}\text{N}$ . In summer, the snow cover almost disappears except in the western part of the TP and the region north of  $70^{\circ}\text{N}$ . In order to study the interannual variability of anomalous snow cover, its standard deviation in spring is calculated. Large standard deviation appears over the Eurasian region from  $45^{\circ}\text{N}$  to  $70^{\circ}\text{N}$  and from  $20^{\circ}\text{E}$  to  $140^{\circ}\text{E}$  (Figure 2). Therefore, this Eurasian region is selected for our study to explore the connection between spring snow cover over Eurasia and EASM.

[8] Figure 3 shows the annual cycle of monthly snow cover over the Eurasian region. The annual cycle is characterized by large values in winter, rapid demise in spring, and almost no snow in summer. The large variation of

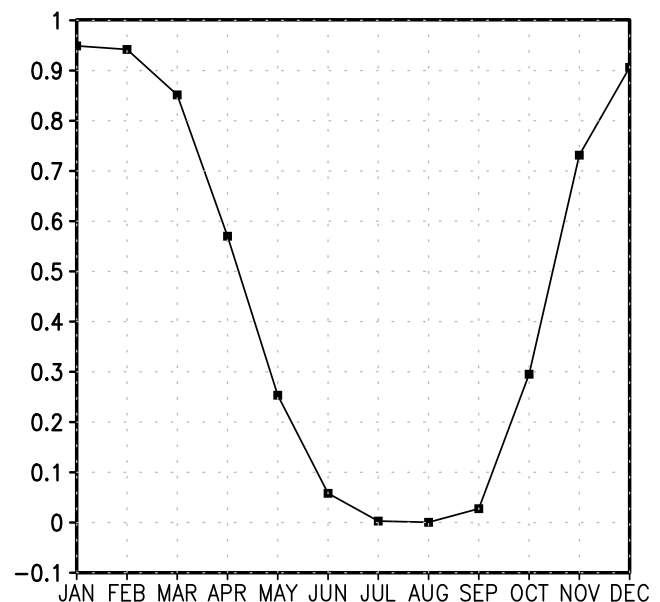


**Figure 3.** The annual cycle of the monthly snow cover averaged over the Eurasian region from  $45^{\circ}\text{N}$  to  $70^{\circ}\text{N}$  and from  $20^{\circ}\text{E}$  to  $140^{\circ}\text{E}$ .

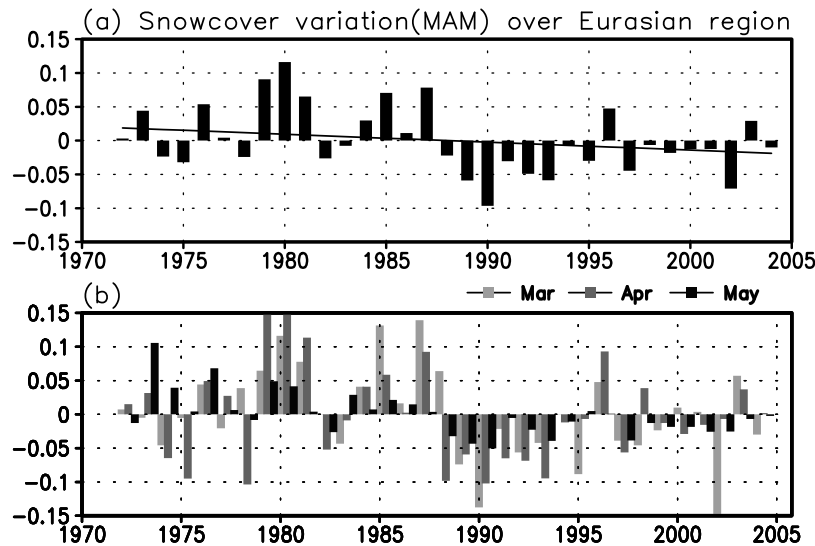


**Figure 4.** The time series of the snow cover anomalies averaged over the Eurasian region in (a) whole spring and (b) each month (March, April, and May) for the period 1972–2004. A straight line in Figure 4a denotes a linear trend of spring snow cover anomaly.

spring snow cover over the Eurasian region could have significant impact on East Asian climate. Figure 4a shows the time series of the spring snow cover anomaly over the Eurasian region. This snow cover anomaly exhibits an apparent decadal change from a positive-anomaly phase to a negative-anomaly phase around the late 1980s and a decreasing trend significant at 95% confidence level. The snow cover anomalies over Eurasia in each month of spring also show similar variations to those in spring (Figure 4b). Maslanik *et al.* [1996] and Tachibana *et al.* [1996] reported that the decadal-scale changes of the Arctic ice cover and sea ice extent in the southern Okhotsk Sea are also shown around the late 1980s. These observational results may describe a large-scale change; therefore, mechanisms of those changes and impacts on EASM need to be further investigated.

#### 4. Two Dominant Modes of Anomalous Spring Snow Cover

[9] In order to identify dominant patterns for anomalous snow cover variability over Eurasia, EOF analysis is performed on the spring snow cover anomalies after removing the linear trend for the period of 1972–2004 (Figure 5). The first and second modes (EOF1 and EOF2) account for about 29% and 16% of the total variance of spring snow cover, respectively (Figures 5c and 5d). The first two leading EOF modes are clearly separated from each other and from the other EOFs according to the criterion of North *et al.* [1982]. EOF1 is characterized by a continent-wide pattern of spring snow cover anomalies over the whole Eurasian region (Figure 5a). In particular, two areas with large loadings are seen over the far western and eastern Eurasia. This pattern (Figure 5a) is quite similar to the distribution of standard deviation for spring snow cover over Eurasia (Figure 2). On the other hand, EOF2 exhibits a dipole pattern over Eurasia, indicating maximum loadings around 60°E and 110°E (Figure 5b). The boundary region between the negative and positive values is around 85°E. The time series of the first

principal component (EOF PC1) indicates decadal variability. On the other hand, the time series of the second principal component (EOF PC2) shows an increase in variance after the late 1980s, suggesting that its contribution to the total variance has been increasing since the late 1980s.

[10] In order to check how much variance is explained by decreasing trend of spring snow cover over Eurasia, the EOF analysis is repeated on the spring snow cover anomaly including the trend (not shown). The result indicates that the first two EOF modes excluding the trend are almost the same as those including the trend, though there are some changes in the variances explained by EOF1 and EOF2. The time series of EOF PC1 including the trend resembles the time series in Figure 4a and exhibits a decreasing trend, which is significant at 95% confidence level. Meanwhile, earlier studies by Kripalani *et al.* [1996] and Dash *et al.* [2005] identified a dipole structure over Eurasia in the first EOF mode of snow depth anomaly only. However, Wu *et al.* [2009] recently showed the EOF modes of snow water equivalent in spring over the area including Eurasia and TP (25°N–80°N, 0°–180°E). The spatial distribution of the first EOF mode represents negative anomalies over Eurasia with the opposite anomalies between the TP and East Asia. The spatial structure of the second EOF mode exhibits opposite variations between western and eastern Eurasian regions, while most of the TP and East Asia have anomalies of the same sign. To compare our results with Wu *et al.* [2009], we have regressed the snow water equivalent anomaly fields during the period 1979–2004 against the time series of the EOF PC1 and the EOF PC2 obtained from an EOF analysis of spring snow cover anomaly over the Eurasian region during the same period. These regressed fields closely resemble the first two EOF modes of spring snow water equivalent from Wu *et al.* [2009] except the TP. That is, the first and the second EOF modes are associated with the continent-wide snow variability and the dipole snow variability of our study, respectively. Although Wu *et al.* [2009]

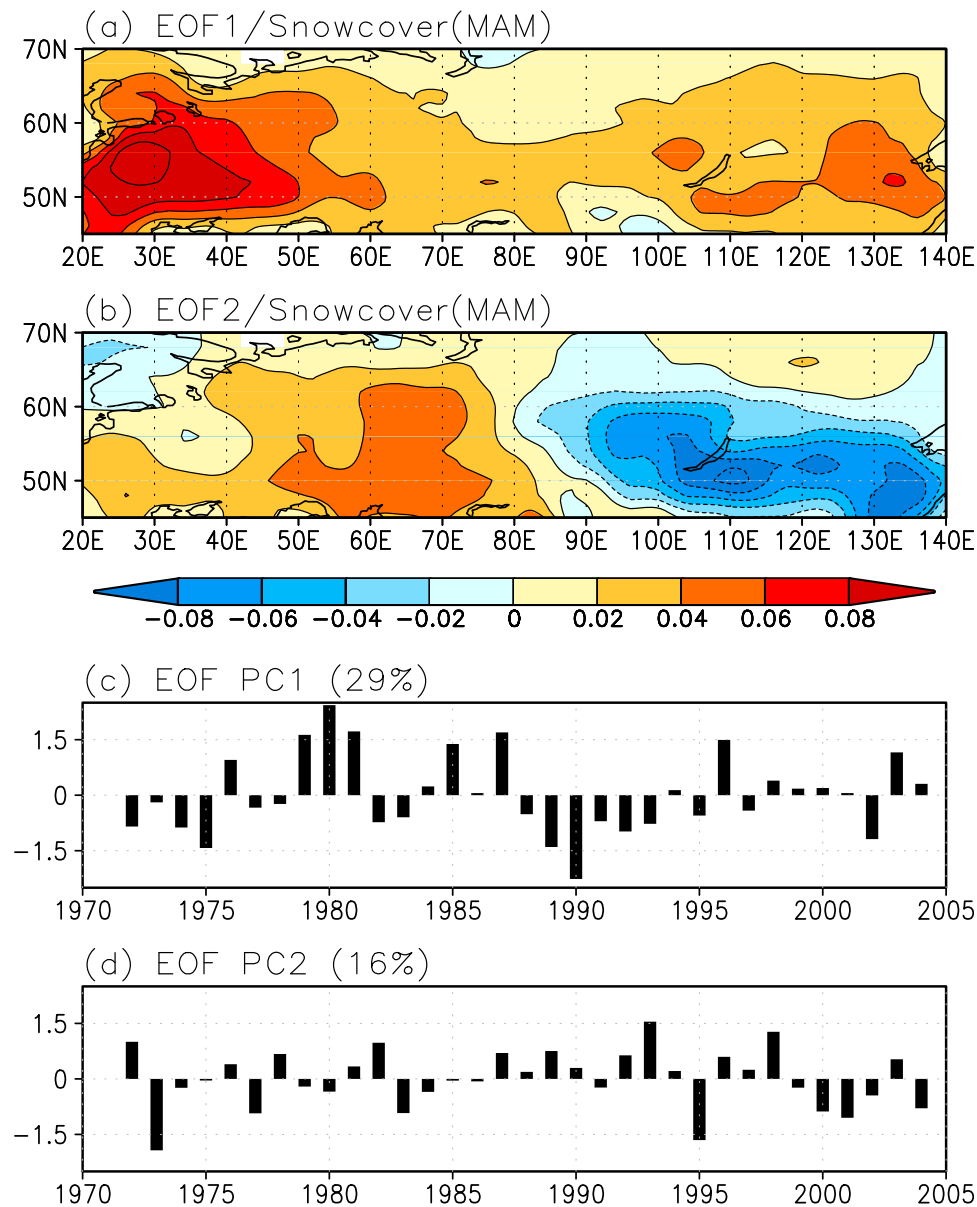


**Figure 5.** (a) First and (b) second EOF modes of snow cover anomaly for the period of 1972–2004. Normalized principal components corresponding to the (c) first and (d) second EOFs.

focused on the Eurasian snow water equivalent variability, they included even the snow water equivalent variability over the TP. Thus, the difference in the snow area between Eurasian region and Eurasian plus TP region may lead to different circulation and rainfall anomaly fields.

[11] On the association with the east-west dipole structure over Eurasia, we investigate the snow cover variability over western Eurasian (hereafter as WEU) region and over the eastern Eurasian (hereafter as EEU) region separately. The time series of the spring snow cover anomaly in the WEU and EEU regions are shown in Figure 6. Here the WEU region is defined as the area from 45°N–60°N and 50°E–75°E and the EEU region as the area from 45°N–60°N and 90°E–140°E. The area of the EEU region is twice that of the WEU region. A remarkable decreasing trend of spring snow cover is found in the EEU region, while no significant trend

exists in the WEU region. We have also examined the horizontal distribution of trend at all grid points. The result indicates significant decreasing trends only over the EEU region (not shown). Thus, the EEU region could be a main contributor to the decreasing trend over Eurasia, although the EEU region does not cover the whole Eurasia. The time series of the difference of spring snow cover between WEU and EEU regions (Figure 6c) is highly correlated to that of the EOF PC2 (Figure 5d) with a correlation coefficient of 0.94, which is significant at 99% confidence level. As described in section 1, previous studies have used the total snow cover averaged over the whole region of Eurasia to understand the snow-monsoon relationship. However, the EOF1 and EOF2 in our study represent the continent-wide pattern and the east-west dipole pattern of snow cover variability, respectively. Thus, it is more instructive to analyze

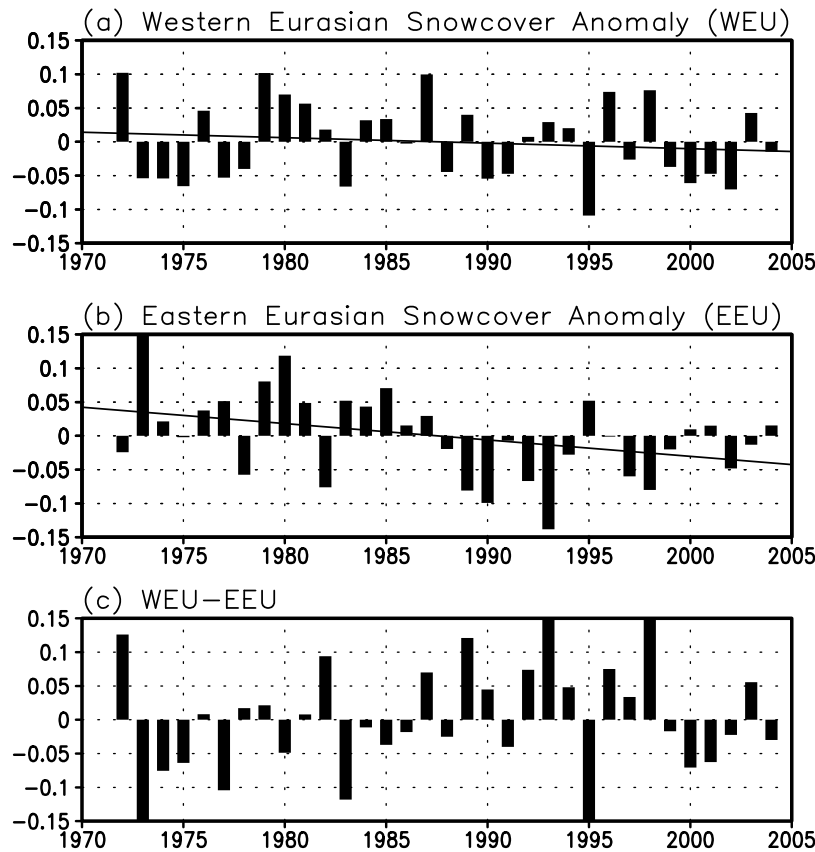


**Figure 6.** Time series of the spring snow cover anomaly over (a) western Eurasian (WEU) and (b) eastern Eurasian (EEU) regions. (c) Difference between Figures 6a and 6b. The straight lines in Figures 6a and 6b denote their linear trends.

the spring snow cover variability in terms of these two leading patterns than to analyze the total snow cover variability.

## 5. Impacts of Two Dominant Modes on the East Asian Climate

[12] In this section, first we search for regions where two dominant modes of the interannual variability in spring snow cover over Eurasian region have apparent correlations with the circulation and the rainfall over the East Asian region. To find such regions, we have calculated the regression fields of the circulation and the rainfall over East Asia in both boreal spring and summer against the time series of two leading EOF modes excluding trends.

### 5.1. Circulations in Spring

[13] The snow cover can exert significant impacts on the regional climate through the following two physical processes. One is that the excessive snow cover in winter and spring may decrease the surface temperature by reducing the net solar radiation at the ground surface through the increase of surface albedo. The other is that the excessive snow cover also gives rise to colder surface temperature because more solar energy is consumed to melt the snow and to evaporate water from the wet soil rather than to heat the ground directly.

[14] Figures 7a and 7b show regressed fields of surface temperature anomaly and geopotential height anomaly at 500 hPa in spring against the time series of EOF PC1. The regressed field of anomalous surface temperature indicates that positive snow cover anomalies over Eurasia correspond to negative surface temperature anomalies over the same Eurasian region (Figure 7a). The teleconnection in 500 hPa geopotential height fields associated with the EOF PC1 is characterized by opposite sign height anomalies between the midlatitudes and the polar region (Figure 7b). This simultaneous teleconnection is similar to an arctic oscillation (AO) pattern [Wallace and Gutzler, 1981]. The AO index denotes the time series of the first EOF mode of 1000 hPa geopotential height anomaly at all longitudes and north of 20°N in winter [Thompson and Wallace, 1998]. The time series of EOF PC1 in our study is correlated to the AO index with the correlation coefficient of  $-0.45$ , which is significant at 95% confidence level. However, the linking mechanisms between the Eurasian snow cover and the AO are not clear yet. On the other hand, the regressed field of surface temperature anomalies in spring against the time series of EOF PC2 displays negative and positive surface temperature anomalies over WEU and EEU regions due to positive and negative snow cover anomalies, respectively (Figure 7c). The high (low) snow cover and the low (high) surface temperature over the WEU (EEU) region correspond to an anomalous cyclone (anticyclone) (Figure 7d).



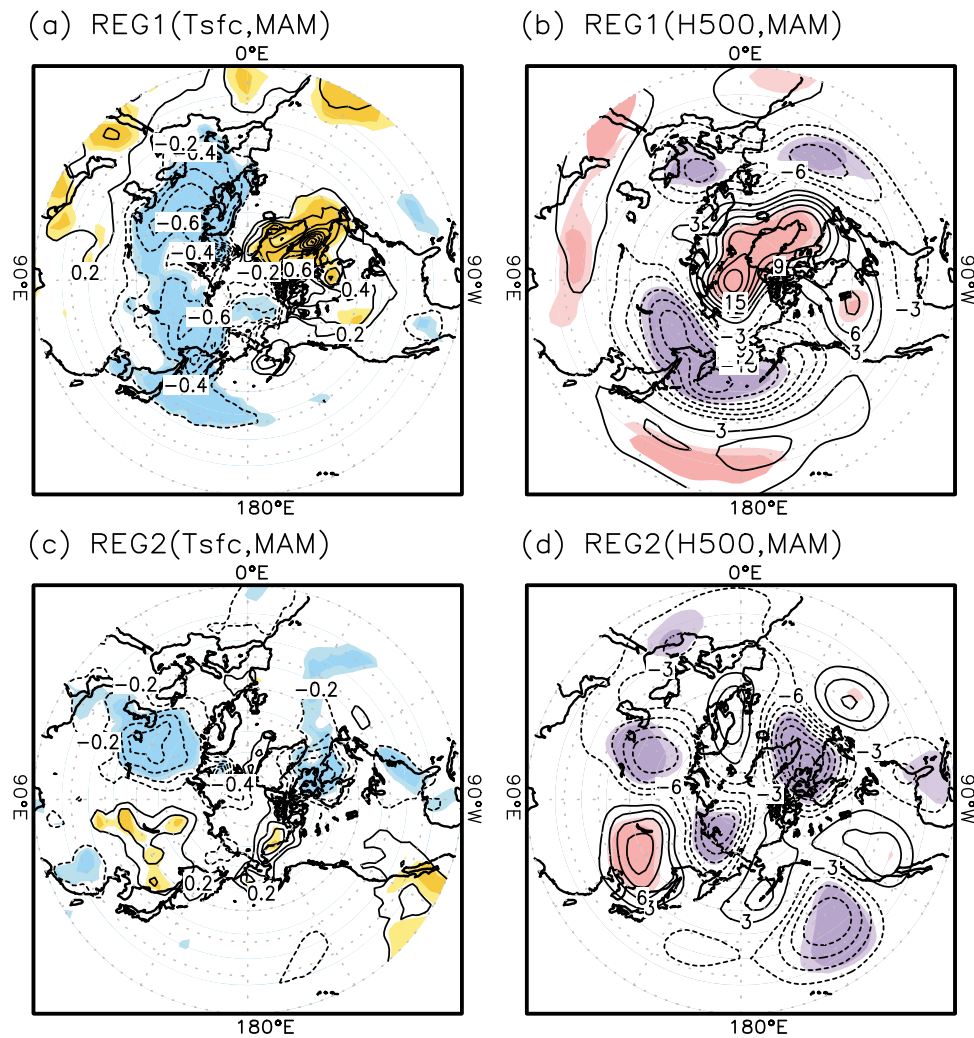


**Figure 7.** Regression of (a) surface temperature (Tsf) and (b) 500 hPa geopotential height (H500) anomalies in spring against the time series of EOF PC1. (c) Same as Figure 7a and (d) same as Figure 7b but for the EOF PC2. The zero contours are removed. The light and dark shadings indicate 90% and 95% confidence levels, respectively.

## 5.2. Rainfall and Circulation in Summer

[15] To investigate delayed impacts on the summer rainfall over East Asia (30°N–45°N, 110°E–145°E) associated with the continent-wide pattern of spring snow cover anomalies over the whole Eurasia, we have regressed the summer precipitation against the time series of EOF PC1. In the regressed summer rainfall pattern associated with the continent-wide snow, localized positive precipitation is seen in southeastern China, southern part of Korea, and northern Japan, with negative precipitation to the south of this wet region (Figure 8a). The regression field of summer 500 hPa geopotential height anomalies shows a prominent anticyclone over the southern part of the East Asian region (Figure 9a), which is consistent with the reduced rainfall over the same region. However, results show that the noticeable correlation regions in Figure 8a are limited to relatively small areas. To confirm these results we have applied the same analysis to the CMAP data for the period 1979–2004 (not shown). The regressed patterns of CMAP anomalies are quite similar

to Figure 8, although locations of maximum regressed anomalies are slightly shifted compared to Figure 8.

[16] On the other hand, in the delayed impacts on the summertime rainfall associated with the dipole pattern snow, positive rainfall anomalies are significant over Korea and Japan, while negative rainfall anomalies are located in the western North Pacific (Figure 8b). This implies that the dipole pattern over Eurasia may be used as a predictor for rainfall variability over the above regions. In the regressed circulation field, compared to the 500 hPa geopotential height anomalies over the western Eurasian and eastern Eurasian regions in spring (Figure 7d), those over above regions in summer have opposite signs (Figure 9b). Interestingly, the regressed temperature anomaly pattern over Eurasia is reversed in summer compared to spring, even though the magnitudes of anomalies in summer are smaller than those in spring. That is, positive and negative surface temperature anomalies appear over the western and eastern Eurasian regions during summer, respectively (not shown). Considering that the regressed 500 hPa geopotential height

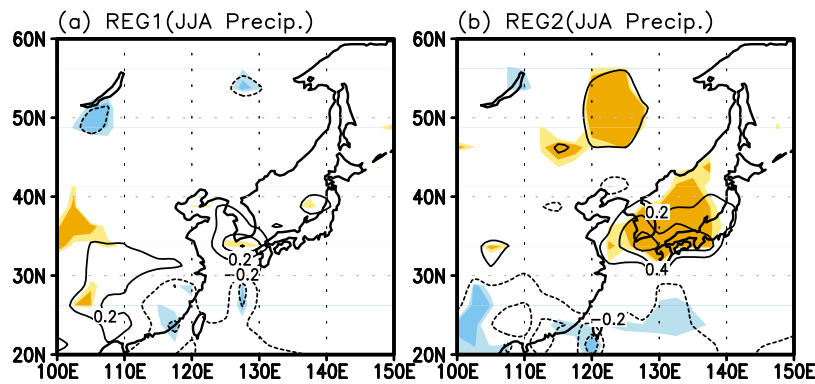


**Figure 8.** Regression of (a) precipitation anomalies in summer against the time series of the EOF PC1. (b) Same as Figure 8a but for the EOF PC2. The zero contours are removed. The light and dark shadings indicate 90% and 95% confidence levels, respectively.

field and the regressed surface temperature field are matched over the Eurasian region in spring (Figures 7c and 7d), the regressed field of 500 hPa geopotential height in summer may be influenced by that of summer surface temperature. The anomalous cyclonic circulation over the East Asian region could enhance the EASM rainfall and is consistent with positive rainfall anomalies over East Asia (Figure 8b).

[17] The summer circulation anomalies at 500 hPa exhibit an apparent wave pattern over the Eurasian continent (EU) (Figure 9b). Interestingly, this resembles an EU pattern. The correlation coefficient between the time series of EOF PC2 and the EU index is 0.45, which is significant at 95% confidence level. The definition of the EU index used in our study is  $-0.25H^*(55^\circ\text{N}, 20^\circ\text{E}) + 0.5H^*(55^\circ\text{N}, 75^\circ\text{E}) - 0.25H^*(40^\circ\text{N}, 145^\circ\text{E})$ , where  $H^*$  denotes the geopotential height anomaly at 500 hPa [Wallace and Gutzler, 1981]. The above results imply that the two modes of spring snow cover over Eurasia may play different roles in affecting summer circulation and rainfall as well as spring circulation over the East Asian region. Our study indicates that the

variability of dipole pattern snow cover is more closely related to the EASM rainfall than that with continent-wide snow cover.

[18] The connection between the spring snow cover and summer rainfall/circulation is difficult to explain because of the time lags involved. However, the dipole pattern of Eurasian snow cover variability in spring may provide a complementary precursor for EASM prediction as described in section 5.2. To assess this possibility, we calculate correlation coefficients between the spring snow cover anomaly and the East Asian summer rainfall anomaly (EASRA) averaged over the EASM region of  $30^\circ\text{N}–45^\circ\text{N}$  and  $115^\circ\text{E}–140^\circ\text{E}$  (Figure 10). The correlation map indicates that a strong EASM is anticipated when significant positive and negative snow cover anomalies over WEU and EEU regions, respectively, exist in spring. Moreover, the correlation coefficient between the EASRA and the EOF PC2 indicating the dipole pattern over Eurasia is 0.5, which is significant at 95% confidence level. Thus, as mentioned in section 5.2, the correlation map supports that the dipole pattern variability of

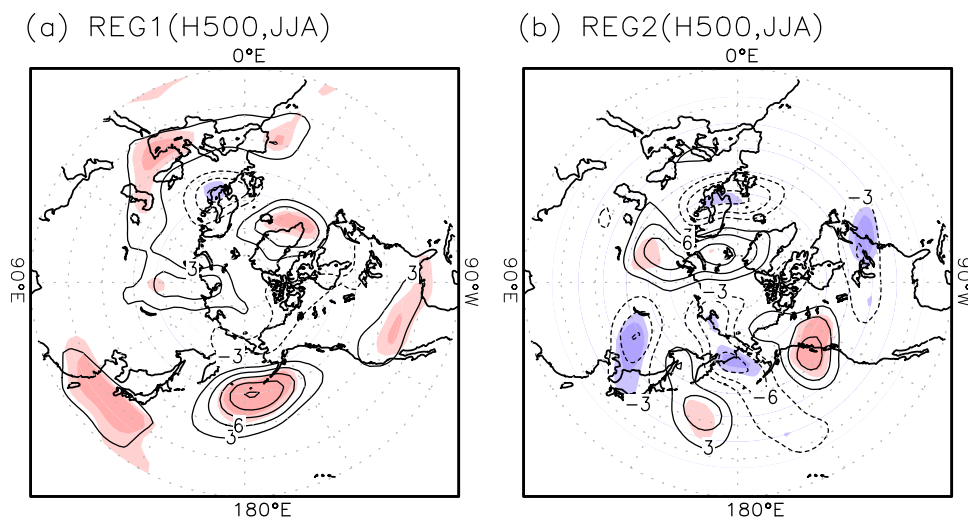


**Figure 9.** Same as Figure 8 but for the 500 hPa geopotential height anomalies.



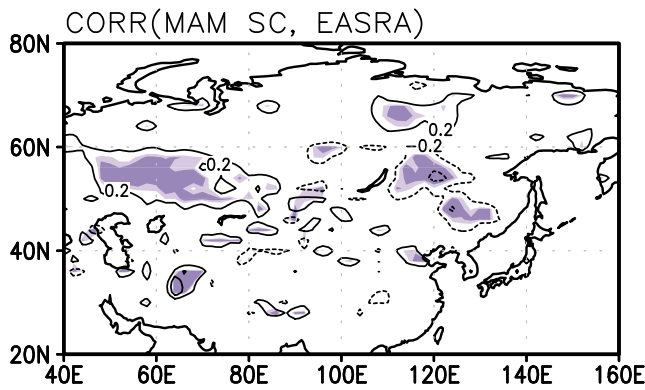


**Figure 10.** The correlation map between the snow cover in spring and the East Asian summer rainfall anomaly (EASRA) averaged over the region ( $30^{\circ}\text{N}$ – $45^{\circ}\text{N}$ ,  $115^{\circ}\text{E}$ – $140^{\circ}\text{E}$ ). The zero contours are removed. The light and dark shadings indicate 90% and 95% confidence levels, respectively.

spring snow cover over Eurasia also could be one of the possible factors affecting the EASM system.

## 6. Summary and Discussions

[19] The seasonal climatology of snow cover distribution shows that the Eurasian region ( $45^{\circ}\text{N}$ – $70^{\circ}\text{N}$ ,  $20^{\circ}\text{E}$ – $140^{\circ}\text{E}$ ) is one of the main snow cover areas. For this region, many previous observational and modeling studies showed that the Eurasian snow cover and snow depth in winter and spring are inversely related to the ISM rainfall. However, in spite of the concern about snow cover variability in winter and spring over Eurasia, its influence on the EASM has not been studied deeply enough so far. In this study, we have investigated spring snow cover variability over the Eurasian region through EOF analysis and simultaneous and delayed impacts of this snow cover variability on atmospheric circulation and rainfall over East Asia. Two distinct structures of spring Eurasian snow cover anomaly are characterized by a continent-wide pattern (EOF1) and an east-west dipole pattern (EOF2). The spring snow cover over Eurasian region tends to decrease and the significant decreasing trend in the EEU region may contribute to the variation over the whole Eurasian region.

[20] In our study, a significant linkage between spring snow cover anomaly over Eurasia and the EASM rainfall has been found. It is noted that east-west dipole pattern variability in spring snow cover is much more closely related to the EASM rainfall than the continent-wide variability. This indicates that the spring snow cover pattern over Eurasia would be a predictor for the EASM rainfall. When spring snow cover anomalies over the western and eastern Eurasia are positive and negative, respectively, the associated summer circulation shows the positive phase of EU pattern at 500 hPa and enhanced summer rainfall over East Asia. Under the positive phase of EU pattern, the anomalous cyclone in the upper levels over East Asia induces cold advection which leads to increase the convective instability over East Asia in the deepened trough. Thus, this EU pattern may give rise to a favorable condition for enhancing precipitation over East Asia. However, the rela-

tionship between the spring snow cover over Eurasia and the summer EU pattern has not been clear so far. In addition, it is very difficult to explain physical mechanisms of delayed impacts of anomalous spring snow cover over the Eurasian region on the EASM rainfall. The more realistic numerical models of the climate system using the realistic snow cover and snow depth are essential to understand the mechanism through which extensive spring snow anomalies over Eurasia would produce deficient or excessive rainfall over East Asia. The physical mechanisms could be obtained by investigations through elaborated simulations in the future.

[21] The El Niño–Southern Oscillation (ENSO) may contribute to or interfere with the snow-monsoon relationship [Wu and Kirtman, 2007]. In order to investigate whether or not two snow cover modes in spring are affected by ENSO, lead-lag correlations between the EOF PCs and the seasonal Niño3 SST indices are calculated (not shown). The Niño3 SST index is defined by SST anomalies averaged over the Niño3 region ( $5^{\circ}\text{S}$ – $5^{\circ}\text{N}$ ,  $150^{\circ}\text{W}$ – $90^{\circ}\text{W}$ ). The continent-wide and east-west dipole snow patterns have no simultaneous correlation with ENSO. Interestingly, the time series of EOF PC1 is not significantly correlated with the seasonal Niño3 SST indices, but EOF PC2 is associated with SST anomalies over the eastern equatorial Pacific in autumn and winter after the appearance of dipole pattern of spring snow cover. This implies that an east-west dipole pattern of spring Eurasian snow cover could predict the ENSO in addition to the EASM rainfall. Thus, because the east-west dipole snow cover is not simultaneously correlated with ENSO, the ENSO may not interfere the relationship between the dipole snow cover variability and the EASM. A clear physical mechanism to connect Eurasian snow cover dipole and ENSO needs to be investigated.

[22] **Acknowledgments.** This work was funded by the Korea Meteorological Administration Research and Development Program under grant CATER 2006–4205 and the National Natural Science Foundation of China under grant 40810059005. This research was also supported by the Japan Agency for Marine-Earth Science and Technology (JAMSTEC), by NASA through grant NNX07AG53G, and by NOAA through grant NA09OAR4320075, which sponsor research at the International Pacific Research Center. This paper is based on IPRC contribution 731 and SOEST contribution 8038. We thank four anonymous reviewers for their constructive comments.

## References

- Bamzai, A. S., and L. Marx (2000), COLA AGCM simulation of the effect of anomalous spring snow over Eurasia on the Indian summer monsoon, *Q. J. R. Meteorol. Soc.*, *126*, 2575–2584, doi:10.1002/qj.49712656811.
- Bamzai, A. S., and J. Shukla (1999), Relation between Eurasian snow cover, snow depth, and the Indian summer monsoon: An observational study, *J. Clim.*, *12*, 3117–3132, doi:10.1175/1520-0442(1999)012<3117:RBESCS>2.0.CO;2.
- Barnett, T. P., L. Dumenil, U. Schlese, E. Roekler, and M. Latif (1989), The effect of Eurasian snow cover on regional and global climate variations, *J. Atmos. Sci.*, *46*, 661–686, doi:10.1175/1520-0469(1989)046<0661:TEOESC>2.0.CO;2.
- Chamey, J., and J. Shukla (1981), Predictability of monsoons, in *Monsoon Dynamics*, edited by J. Lighthill and R. P. Pearce, pp. 99–109, Cambridge Univ. Press, Cambridge, U. K.
- Chen, L.-T., and R. Wu (2000), Interannual and decadal variations of snow cover over Qinghai-Xizang Plateau and their relationships to summer monsoon rainfall in China, *Adv. Atmos. Sci.*, *17*, 18–30, doi:10.1007/s00376-000-0040-7.
- Chen, M., P. Xie, J. E. Janowiak, and P. A. Arkin (2002), Global land precipitation: A 50-yr monthly analysis based on gauge observations,

- J. Hydrometeorol.*, 3, 249–266, doi:10.1175/1525-7541(2002)003<0249:GLPAYM>2.0.CO;2.
- Dash, S. K., G. P. Singh, M. S. Shekhar, and A. D. Vernekar (2005), Response of the Indian summer monsoon circulation and rainfall to seasonal snow depth anomaly over Eurasia, *Clim. Dyn.*, 24, 1–10, doi:10.1007/s00382-004-0448-3.
- Dash, S. K., M. S. Shekhar, and G. P. Singh (2006a), Simulation of Indian summer monsoon circulation and Rainfall using RegCM3, *Theor. Appl. Climatol.*, 86, 161–172, doi:10.1007/s00704-006-0204-1.
- Dash, S. K., P. P. Sarthi, and S. K. Panda (2006b), A study of the effect of Eurasia snow on the summer monsoon circulation and rainfall using a spectral GCM, *Int. J. Climatol.*, 26, 1017–1025, doi:10.1002/joc.1299.
- Hahn, D. J., and J. Shukla (1976), An apparent relationship between Eurasian snow cover and Indian monsoon rainfall, *J. Atmos. Sci.*, 33, 2461–2462, doi:10.1175/1520-0469(1976)033<2461:AARBES>2.0.CO;2.
- Kalnay, E., et al. (1996), The NCEP/NCAR 40-Year Reanalysis Project, *Bull. Am. Meteorol. Soc.*, 77, 437–471, doi:10.1175/1520-0477(1996)077<0437:TNYRP>2.0.CO;2.
- Kripalani, R. H., S. V. Singh, A. D. Vernekar, and V. Thapliyal (1996), Empirical study on Nimbus-7 snow mass and Indian summer monsoon rainfall, *Int. J. Climatol.*, 16, 23–34, doi:10.1002/(SICI)1097-0088(199601)16:1<23::AID-JOC988>3.0.CO;2-J.
- Kripalani, R. H., S. V. Singh, A. D. Vernekar, and V. Thapliyal (2002), Relationship between Soviet snow and Korean rainfall, *Int. J. Climatol.*, 22, 1313–1325, doi:10.1002/joc.809.
- Kripalani, R. H., A. Kulkarni, and S. S. Sabade (2003), Western Himalayan snow cover and Indian monsoon rainfall: A re-examination with INSAT and NCEP/NCAR data, *Theor. Appl. Climatol.*, 74, 1–18, doi:10.1007/s00704-002-0699-z.
- Liu, X., and M. Yanai (2002), Influence of Eurasian spring snow cover on Asian summer rainfall, *Int. J. Climatol.*, 22, 1075–1089, doi:10.1002/joc.784.
- Maslanik, J. A., M. C. Serreze, and R. G. Barry (1996), Recent decreases in Arctic summer ice cover and linkages to atmospheric circulation anomalies, *Geophys. Res. Lett.*, 23, 1677–1680, doi:10.1029/96GL01426.
- North, G. R., T. L. Bell, R. F. Cahalan, and F. J. Moeng (1982), Sampling errors in the estimation of empirical orthogonal functions, *Mon. Weather Rev.*, 110, 699–706, doi:10.1175/1520-0493(1982)110<0699:SEITEO>2.0.CO;2.
- Sankar-Rao, M., K. M. Lau, and S. Yang (1996), On the relationship between Eurasian snow cover and the Asian summer monsoon, *Int. J. Climatol.*, 16, 605–616, doi:10.1002/(SICI)1097-0088(199606)16:6<605::AID-JOC41>3.0.CO;2-P.
- Tachibana, Y., M. Honda, and K. Takeuchi (1996), The abrupt decrease of the sea ice over the southern part of the sea of Okhotsk in 1989 and its relation to the recent weakening of the Aleutian low, *J. Meteorol. Soc. Jpn.*, 74, 947–954.
- Thompson, D. W. J., and J. M. Wallace (1998), The Arctic oscillation signature in the wintertime geopotential height and temperature fields, *Geophys. Res. Lett.*, 25, 1297–1300, doi:10.1029/98GL00950.
- Wallace, J. M., and D. S. Gutzler (1981), Teleconnections in the geopotential height field during the Northern Hemisphere winter, *Mon. Weather Rev.*, 109, 784–812, doi:10.1175/1520-0493(1981)109<0784:TITGHF>2.0.CO;2.
- Wu, B. Y., K. Yang, and R. H. Zhang (2009), Eurasian snow cover variability and its association with summer rainfall in China, *Adv. Atmos. Sci.*, 26, 31–44, doi:10.1007/s00376-009-0031-2.
- Wu, R., and B. P. Kirtman (2007), Observed relationship of spring and summer East Asian rainfall with winter and spring Eurasian snow, *J. Clim.*, 20, 1285–1304, doi:10.1175/JCLI4068.1.
- Wu, T.-W., and Z.-A. Qian (2003), The relation between the Tibetan winter snow and the Asian summer monsoon and rainfall: An observational investigation, *J. Clim.*, 16, 2038–2051, doi:10.1175/1520-0442(2003)016<2038:TRBTTW>2.0.CO;2.
- Xie, P., and P. A. Arkin (1997), Global precipitation: A 17-year monthly analysis based on gauge observations, satellite estimates, and numerical model outputs, *Bull. Am. Meteorol. Soc.*, 78, 2539–2558, doi:10.1175/1520-0477(1997)078<2539:GPAYMA>2.0.CO;2.
- Yang, S., and L. Xu (1994), Linkage between Eurasian winter snow cover and regional Chinese summer rainfall, *Int. J. Climatol.*, 14, 739–750, doi:10.1002/joc.3370140704.
- Yasunari, T., A. Kitoh, and T. Tokioka (1991), Local and remote responses to excessive snow mass over Eurasia appearing in the northern spring and summer climate—A study with the MRI-GCM, *J. Meteorol. Soc. Jpn.*, 69, 473–487.
- Zhang, Y., T. Li, and B. Wang (2004), Decadal change of the spring snow depth over the Tibetan Plateau: The associated circulation and influence on the East Asian summer monsoon, *J. Clim.*, 17, 2780–2793, doi:10.1175/1520-0442(2004)017<2780:DCOTSS>2.0.CO;2.
- Zhao, P., Z. Zhou, and J. Liu (2007), Variability of Tibetan spring snow and its associations with the hemispheric extratropical circulation and East Asian summer monsoon rainfall: An observational investigation, *J. Clim.*, 20, 3942–3954, doi:10.1175/JCLI4205.1.

J.-G. Jhun, School of Earth and Environmental Sciences, Seoul National University, 599 Gwanangno, Gwanak-gu, Seoul 151-747, South Korea. (jgjhun@snu.ac.kr)

R. Lu, Institute of Atmospheric Physics, Chinese Academy of Sciences, Beijing 100029, China.

B. Wang, International Pacific Research Center, University of Hawai'i at Manoa, Honolulu, HI 96822, USA.

S.-Y. Yim, Research Institute of Basic Sciences, Seoul National University, Seoul 151-747, South Korea.